

IMPROVED TECHNIQUES FOR ASSESSING RIDE QUALITY ON CONCRETE PAVEMENTS

Hans Prem¹, BE(Mech), PhD, FIEAust
Geoff Ayton², BE(Civil), MIEAust

Abstract

Under current procedures used in Australia for testing and interpretation of road profiles it is difficult to identify and isolate pavement sections responsible for unpleasant ride vibration. For the construction of new concrete pavements, in particular, where subsequent correction of profiles is very expensive, there is a need for improved procedures to give early feedback of the ultimate ride quality. To help identify and treat pavement problem areas, numerical models were developed to simulate ride vibration and pavement grinding. The ride and grind simulation models cover four generic vehicle classes – passenger cars, heavy commercial vehicles, off-road recreational and sports utility vehicles and motorcycles – and conventional pavement grinding equipment. A number of vibration response presentation formats were developed to help quantify ride vibration severity, intrinsic unevenness and grind treatment effectiveness. The models and key findings of the study are presented in this paper through contrasting examples of responses from the models to a selection of road profiles before and after virtual (theoretical) remedial grind treatment.

Introduction

Consistent with road user expectations, the Roads and Traffic Authority of New South Wales (RTA) in Australia is seeking to improve the standard of ride quality on its road network. Current procedures for testing and interpretation of road profiles to identify and isolate sections of pavement responsible for unpleasant ride vibration have met with mixed success. For example, isolated sections that are flagged as “must grind” sometimes prove to be satisfactory to road users and hence do not warrant grinding. Conversely, sections that have not been identified as requiring grinding will sometimes prove to be uncomfortable to road users. For the construction of new concrete pavements, in particular, where subsequent correction of profiles is very expensive, there is a need for improved procedures that will give early feedback to construction staff of the ultimate ride quality.

¹ Director and Senior Consultant, Mechanical System Dynamics Pty Ltd, 14 Browning Drive, Templestowe, Victoria 3106, AUSTRALIA, email: hansprem@iprimus.com.au, ph: +61 3 9841 6485, fx: +61 3 9841 4363.

² Manager, Rigid Pavements, Roads & Traffic Authority of NSW, 85 Flushcombe Road, Blacktown, NSW 2148, AUSTRALIA, email: geoff_ayton@rta.nsw.gov.au, ph: +61 2 8814 2573, fx: 8814 2312.

To address the above issues, some basic profile analysis tools were developed together with numerical models to simulate ride vibration in four generic road-user vehicle classes – passenger cars, heavy commercial vehicles (trucks), off-road recreational and sports utility vehicles (SUVs) and motorcycles. To facilitate analysis of discrete sections of profiles recorded with a range of profiling equipment, and to clearly identify pavement problems areas, a number of presentation formats were developed and considered. To further assist the process, numerical models were also developed to simulate conventional pavement grinding equipment so that virtual remedial treatments could be applied to the profile and potential improvements in rideability determined and evaluated.

This paper introduces the analysis tools, the ride and pavement grinding numerical models, and the underlying concepts and background to them. The tools and models are demonstrated, and the key findings of the study are presented through contrasting examples of vibration responses to a selection of road profiles before and after remedial grind treatments have been applied.

Research and Practical Significance

A number of fundamental issues associated with the measurement and interpretation of road roughness and its relationship to pavement rideability are considered.

Traditional mechanical response-type road roughness measuring systems, and road profile measuring systems that either simulate response-type systems or characterise some geometric aspects of a profile, only provide indirect indications of pavement ride quality in passenger cars established through correlation studies. Consequently, when considered across a broad range of vehicle classes and road users, road roughness measurements frequently do not correlate with subjective ratings of pavement rideability.

The generic ride model developed and presented in this paper closely replicates the actual ride responses of four very different vehicle classes and their occupants. As a result, the model is sensitive to profile unevenness and specific features not detected by traditional roughness measures. Therefore, the outcome of this research is a new pavement rideability indicator and a wide range of ride quality estimates covering a board range of vehicle classes and road users, which can be directly linked to subjective ratings of pavement induced in-vehicle ride vibration.

The ride models, together with the profile grinding and analysis tools presented in this paper, are expected to help improve road paving operations and targeting of profile remediation activities both in new and existing rigid and flexible pavements.

Profile Analysis Tool

The ability and ease with which specific problem areas of new or existing pavements can be located and isolated is related to the nature of the specific profile feature and to the survey report interval. In Australia, road roughness measurements³ are reported as average values over 100 m intervals for both general surveys and for construction control (Roads and Traffic Authority, 2002a; Austroads, 2001). Over this reporting interval, a discrete feature occurring within a short distance, such as a paving construction joint or bridge abutment, while easy to locate, could have an influence on the section unevenness value similar to that of a less obvious rough patch that extends over a much longer distance. Further, subtle changes in unevenness characteristics would not always be apparent over long reporting intervals.

Some basic tools were developed to show how bumps and rough areas of a profile contribute incrementally and on a profile point-by-point basis to the overall development of the final unevenness value. Two measures were developed and tested to help identify and isolate pavement problem areas. The first draws on some basic features of response-type road roughness measuring systems, as reflected in the International Roughness Index (IRI)⁴ (Sayers et al, 1986), and the second is a direct application of the ride vibration measure described later in this paper.

International Roughness Index. In its simplest form the IRI can be described as a mathematical transform of the measured profile. Conceptually it can be thought of as a “quarter-car” representation of a road roughness measuring system, comprising a vehicle and a road roughness meter that measures the relative motion response between a vehicle’s sprung and unsprung masses to road profile, as illustrated schematically in the sequence shown in Fig. 1.

In the IRI, relative movement between the sprung and unsprung masses causes roughness displacement to be generated and accumulated in the “meter”. At the end of a test section the accumulated displacement is simply divided by the length of the section yielding a roughness measure that is expressed in units of axle-to-body displacement per unit of distance travelled; m/km for standard IRI measurements.

IRI Roughness Accumulator. More formally, the IRI is an accumulation of the simulated motion between the sprung and unsprung masses in the standard quarter-car model of Fig. 1, normalised by the length, L , of the profile (Sayers, 1995). It is expressed mathematically as:

$$IRI = \frac{1}{L} \int_0^{L/V} \left| \dot{z}_s - \dot{z}_u \right| dt \quad (1)$$

³ Based on NAASRA Roughness, a vehicle response-type measure similar to the IRI (Prem, 1989a).

⁴ Although the IRI is used throughout this paper, the Australian equivalent measure, NAASRA Roughness, and the IRI are conceptually identical (Prem, 1989a). The findings presented in this paper are equally applicable to both the IRI and NAASRA Roughness.

where:

- \dot{z}_s = Vertical velocity of the quarter-car sprung mass (m/s)
- \dot{z}_u = Vertical velocity of the quarter-car unsprung mass (m/s)
- L = Length of the profile (m)
- V = Simulated forward speed (m/s)
- dt = Small increment of time (s), as defined by the definite integral.

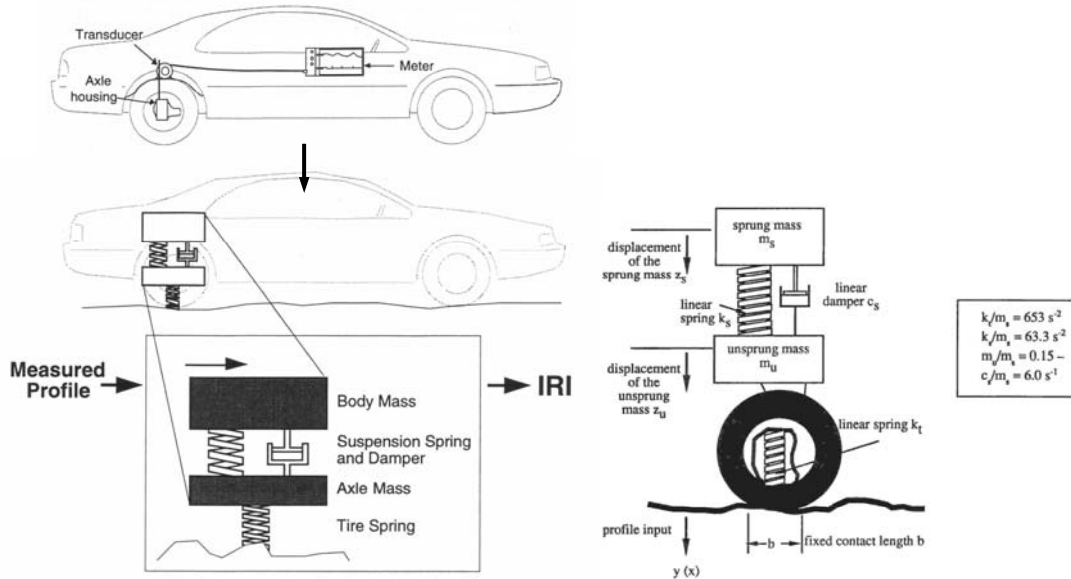


Figure 1. Quarter-car representation of the IRI (from Sayers and Karamihas, 1998)

The difference between the quarter-car sprung and unsprung mass velocities given in Eqn (1) is referred to as the axle-body relative velocity, and is analogous to the relative vertical velocity between the centre of rear-axle housing and the sprung mass of a real vehicle. This relative velocity has a zero average value over the distance (or time) interval of interest. To determine the accumulated axle-body movement, the axle-body relative velocity values are first all made positive in Eqn (1) by taking the absolute values, and then numerically integrated over the time interval that it takes to travel the length of the profile, L , at the simulated travel speed, V . In Eqn (1) the time interval is set by the limits of integration, which is from time $t = 0$ to L/V . For the IRI the travel speed is set to a fixed value of 80 km/h.

To compute the IRI, the accumulated axle-body movement is simply divided by the length of the profile, L . For convenience the components of Eqn (1) are summarised below in Table 1.

The two parameters shown in Table 1 of prime interest to this paper, and explored further below, are quantities #5 and #6; the accumulated axle-body movement (AABM) and the IRI.

Table 1. Description of Eqn (1) quantities

#	Quantity	Description	Units
1	\dot{z}_s	Vertical velocity of the sprung mass.	m/s
2	\dot{z}_u	Vertical velocity of the unsprung mass.	m/s
3	$\dot{z}_s - \dot{z}_u$	Relative velocity between the sprung and unsprung masses.	m/s
4	$ \dot{z}_s - \dot{z}_u $	Absolute value of the relative velocity.	m/s
5	$\int_0^{L/V} \dot{z}_s - \dot{z}_u dt$	Accumulated axle-body movement measured over profile length L (roughness accumulation).	m (or mm)
6	$\frac{1}{L} \int_0^{L/V} \dot{z}_s - \dot{z}_u dt$	Accumulated axle-body movement normalised by profile length L . For the standard quarter-car model this is the International Roughness Index (IRI).	m/km (or mm/m)

Application. RTA supplied road profiles of Continuously Reinforced Concrete (CRC) pavement were measured on the Federal Highway at Lake George in New South Wales, Australia, with an ARRB Transport Research Ltd (ARRB) Walking Profiler (WP) (Auff et al, 1995). Software was developed to simulate the motion of the IRI quarter-car model to the measured profiles and the two roughness measures described above, AABM and IRI, were computed.

The response outputs from the simulations showing both the AABM and the instantaneous IRI along a 2250 m section of one of the measured profiles are shown below in Fig. 2. The IRI profile is seen to rise abruptly initially and then vary between values of between about 0.9 to 1.1 m/km, with a final value of about 1.1 m/km at 2200 m, which is the overall IRI value for the entire section. This value of IRI falls within the range of values for airport runways and superhighways and would be considered to be very smooth.

The variation in the IRI profile shown in Fig. 2, exhibiting several abrupt step changes, initially large, at locations shown circled in the plot, is a result of abrupt changes in unevenness along the profile, such as would be due to discrete imperfections, paving construction joints, rough patches, or similar. For profiles having uniform roughness characteristics along the entire length, with no imperfections, the IRI profile would have a smooth, nominally constant value.

The AABM profile shown in Fig. 2 exhibits similar abrupt changes at the same locations, that are more consistent in magnitude, but these are superimposed on a steady increase in accumulation of axle-body movement with distance. The sections of constantly increasing AABM with distance, between the abrupt sections circled in Fig. 2, is referred to herein as *intrinsic unevenness*, and is related to the paving process, reflecting the characteristics of the equipment and its operation (stop/start activities, paving speed), material properties, environmental factors

(temperature and humidity) and a range of other possible influences. This aspect of the paving process and the AABM profile is more fully explored towards the end of this paper.

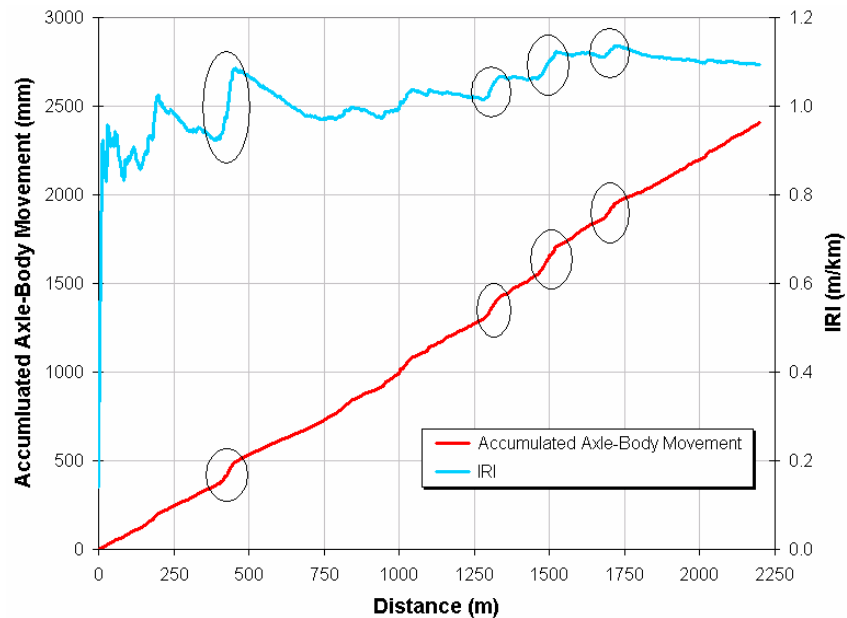


Figure 2. Various IRI responses to Lake George profiles.

Improved Ride Model

The traditional measures of road surface unevenness, such as the IRI described above, measure the vibration response between the vehicle's rear-axle and body. This measures a physical quantity that is fundamentally quite different to ride vibration, which is occurring at another location in the vehicle some distance away, and perceived by the occupants through areas where they have physical contact with the vehicle. Therefore, response-type road roughness measures such as the IRI can be expected to only provide indirect indications of ride quality. Furthermore, as the unevenness measurements have traditionally been taken in passenger cars and correlated through studies with subjective highway user ratings (Al-Omari and Darter, 1994), ride quality indications would only apply to the same specific class of vehicle used in those studies.

More realistic ride quality estimates of road pavements can be obtained by more closely simulating actual vehicle ride dynamics. To do this requires a more complete and thorough understanding of the mechanical properties and dynamics of the whole vehicle, the dynamic properties and isolation characteristics of seating, whole-body biodynamics of the vehicle's seated occupants, and an understanding of human tolerance to whole-body vibration. These four key elements were combined to develop a generic ride model that would more closely replicate the ride responses of a range of different vehicle classes and road users. The outputs from these models would be expected to produce realistic estimates of ride quality that would correlate

well with subjective ratings of pavement rideability. The ride model is presented in the following sections of this paper and demonstrated through specific applications.

Model Description. A schematic of the numerical model for simulating ride vibration is shown in Fig. 3. Generic in form, it can be used to represent any two-axle vehicle having freedom in bounce and pitch travelling along a single wheelpath profile. In the work described in this paper, the model was used to simulate the ride responses of a generic passenger car, a heavy commercial vehicle (truck), an off-road recreational and sports utility vehicle (SUV), and a motorcycle.

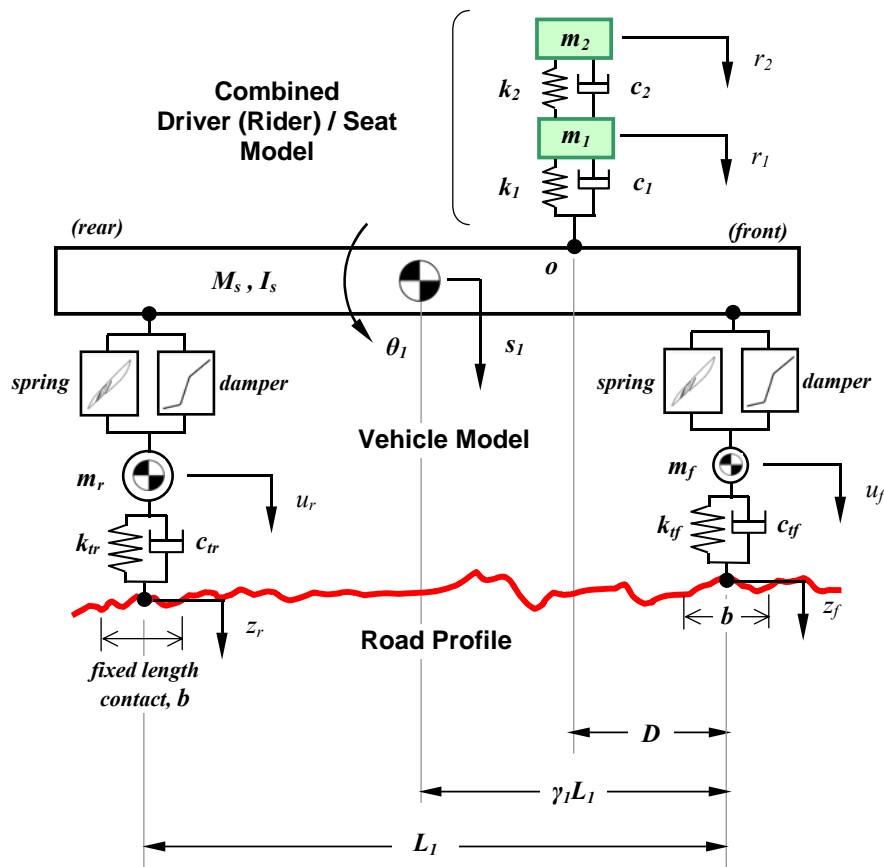


Figure 3. Generic 2-axle ride model.

a) Vehicle. In the model, contact between the two tyres, having vertical stiffness and damping, k_t and c_t , respectively, and the road surface, occurs at two points, z_f and z_r , through a tyre-enveloping model incorporating the fixed length contact, b , over the vehicle wheelbase, L_1 . The tyre-enveloping model is similar to that implemented and used in the IRI quarter-car model (shown in Fig. 1), however, both the tyre mechanical properties (stiffness and damping) and the fixed-length contact length are vehicle specific and need to be determined for each particular vehicle considered. The tyres are connected to the front and rear unsprung masses, m_f and m_r , which have bounce freedom defined by the generalised co-ordinates u_f and u_r , respectively. The

unsprung masses are connected to the sprung mass through the suspension non-linear spring and damper elements. The vehicle's sprung mass, having mass, M_s , and mass moment of inertia in pitch, I_s , is supported on the suspension spring and damper elements and has freedom to move in bounce and pitch, defined by the generalised co-ordinates s_I and θ_I , respectively.

b) Seat/Operator. Connected to the sprung mass, at point O , is a lumped parameter two-mass spring-damper system that represents the vertical-axis mechanical impedance of the combined seat and seated driver (or cushion and rider, for simulation of motorcycle ride dynamics). Ride vibration transmitted by the vehicle to the seat and seated occupant occurs at Point O . This point is taken as the location along the vehicle wheelbase where the vibration enters the human body from the seat cushion at the principal contact area. Hand-arm and foot vibration do not feature in the ride model, though in some applications these may be significant. For the four vehicles considered, three separate generic parameter sets were developed to represent the combined seat/occupant, as described above, based on published data. These were selected to represent "middle-of-the-range" trucks, cars/SUVs and motorcycles.

c) Vibration Perception and Tolerance. The perception and evaluation of ride deals principally with understanding of the relationship between exposure to whole-body vibration and comfort. Many factors contribute to determine the feeling of well being in an individual and vibration is just one of these factors. In the context of this paper, it has been assumed that vibration is the main source of discomfort to a vehicle's occupants. Discomfort due to factors other than vibration, such as noise and heat, has not been considered, though in some environments these may be significant.

The evaluation of ride quality must deal with the complex issue of human tolerance to whole-body vibration. A large number of studies have been conducted over the years dealing with this issue in both ground and air transportation vehicles. Early studies were concerned primarily with the effects of varying vibration along a single axis; others have investigated complex conditions, including multiple-frequency vibration, multiple-axis vibration and shock, and the interaction between noise and vibration (Leatherwood, et. al., 1980; Griffin, 1990).

d) Vibration Standards. Guidance for the assessment of the effects of vibration exposure on health, comfort and perception, as used in the ride model, can be found in International Standard ISO 2631-1 and British Standard BS 6841 (International Standards Organisation, 1997; British Standards Institution, 1987) for seated, standing and reclining persons. The guidance concerns translational and rotational vibration in the frequency range 0.5 to 80 Hz transmitted from a solid surface to the point of entry of vibration to the body.

The magnitude of the vibration exposure is characterised by the *root-mean-square (rms) frequency-weighted acceleration* calculated in accordance with the following equation:

$$a_w = \left[\frac{1}{T} \int_0^T a_w^2(t) dt \right]^{1/2} \quad (2)$$

where $a_w(t)$ is the frequency weighted acceleration, or angular acceleration (for rotation), at time t expressed in metres per second squared (m/s^2), or radians per second squared (rad/s^2), respectively; and T is the duration of the measurement in seconds.

The frequency weightings to be employed for different applications can be found in ISO 2631-1 and BS 6841. In the present application, the principal weighting to be applied for the assessment of the effects of vibration on a seated person in a vehicle (car, SUV, truck or motorcycle) is for vertical vibration at point O due to bounce motions and pitch rotations of the vehicle sprung mass.

e) Ride Quality Measure. The ride quality indicator used in this application is a direct measure of the major component of ride vibration that is responsible for discomfort due to whole-of-body vertical motions. The ride measure is based on estimation of vertical vibration at the point where it enters the body from the seat cushion at the principal contact area. The primary quantity for expressing vibration magnitude is the frequency-weighted root-mean-square (*rms*) acceleration for vertical (z -direction) translational vibration, a_{zw} , defined above in Eqn (2).

The vertical acceleration-based ride indicator outlined above is considered a more transparent and direct measure of the road users' vibration environment than traditional ones used in pavement analysis. It provides, in literal interpretation, a "seat-of-the-pants" measure of ride quality. It is expected to agree closely with road user perception and subjective ratings of ride across a wide range of vehicle classes.

Probable subjective reactions of persons to whole-body vibration in public transportation taken from the standards are listed below in Table 2. It is useful to note that fifty percent of alert, sitting or standing, healthy persons can detect vertical vibration with a frequency weighted acceleration of 0.015 m/s^2 .

Table 2. Likely reactions of seated persons to various levels of a_{zw} acceleration (from ISO 2361-1 and BS 6841)

$a_{zw} \text{ (m/s}^2\text{)}$	Reaction
< 0.315	not uncomfortable
0.315 – 0.63	a little uncomfortable
0.5 – 1.0	fairly uncomfortable
0.8 – 1.6	uncomfortable
1.25 – 2.5	very uncomfortable
> 2.0	extremely uncomfortable

Ride Quality and Pavement Unevenness

In order to test both the qualitative and quantitative significance of the ride quality estimates, simulations were performed using the custom developed *PaveRide*TM software and outputs from the four models were produced and compared to the IRI. The comparisons were made using road profiles collected with an ARRB WP on 10 sections of flexible pavement each nominally 600 m in length. The test sections selected for the comparisons are used routinely to verify and check high-speed road profilers and provide both a large spread of IRI values and a large source of data.

A selection of nominal parameter values used in the ride model to represent the four vehicle classes is given Table 3. Almost 30 parameters are necessary to fully define each ride model. The parameters for each of the four models were obtained from a very large number of different sources both in the public domain (published papers and research reports) and supplied to the project from private industry sources, such as research organisations and vehicle manufacturers. The data sets for each vehicle class were merged to produce a generic set that does not represent any particular make, brand or size of vehicle, the intention being to simply reproduce the response characteristics of an “average” vehicle in each class.

Table 3. Selection of parameter values for the four ride models

Parameter	Motorcycle	Car	SUV	Truck
Gross Mass (kg), $M_s+m_f+m_r$	270	1,650	1,890	12,000
Wheelbase (m), L	1.45	2.75	2.70	4.72
Location of Point O (m), D	1.00	1.25	1.35	0.20
Front Spring Stiffness (N/m)	12,000	46,000	72,500	450,000
Rear Spring Stiffness (N/m)	26,500	53,750	60,000	635,000
Front Tyre Stiffness (N/m), k_{tf}	100,000	450,000	490,000	1,575,000
Rear Tyre Stiffness (N/m), k_{tr}	130,000	450,000	490,000	3,150,000

The spread of ride values from the four ride models is compared to the IRI in Fig. 4 together with the limiting values of ride vibration from the international standards given above in Table 2. The ride models indicate the highest ride vibration levels will generally occur on motorcycles, causing ratings of “uncomfortable” on pavements having IRI levels greater than 3.0 m/km, and “very uncomfortable” on the roughest pavement having an IRI approaching 7.0 m/km.

Fig. 4 shows the truck has the greatest spread in ride values, at times being worse than the motorcycle and at other times no worse than the SUV. The results also show that truck ride can sometimes be better on a pavement having a higher IRI than on one with a lower IRI, consistent with anecdotal evidence reported in Austroads (2000). This suggests that the truck is responding to something in the profile that the IRI is not sensitive to.

The smoothest ride is for the car and generally slightly worse for the SUV, consistent with public reports of the ride quality of these two vehicle classes.

Fig. 4 shows that on the roughest pavement sections (IRI levels greater than 6.5 m/km) the range of likely reactions across all four vehicle classes would be from “fairly uncomfortable” to “very uncomfortable”, and on pavements having roughness values of about 4.0 m/km the likely reaction would be “a little uncomfortable” to “uncomfortable”. In Australia, suggested terminal roughness values for minor urban roads and high standard roads (highways) are about 6.5 m/km and 4.0 m/km IRI, respectively (Austroads, 1992). The predictions from the ride model described above are considered to be largely consistent with the Austroads guide.

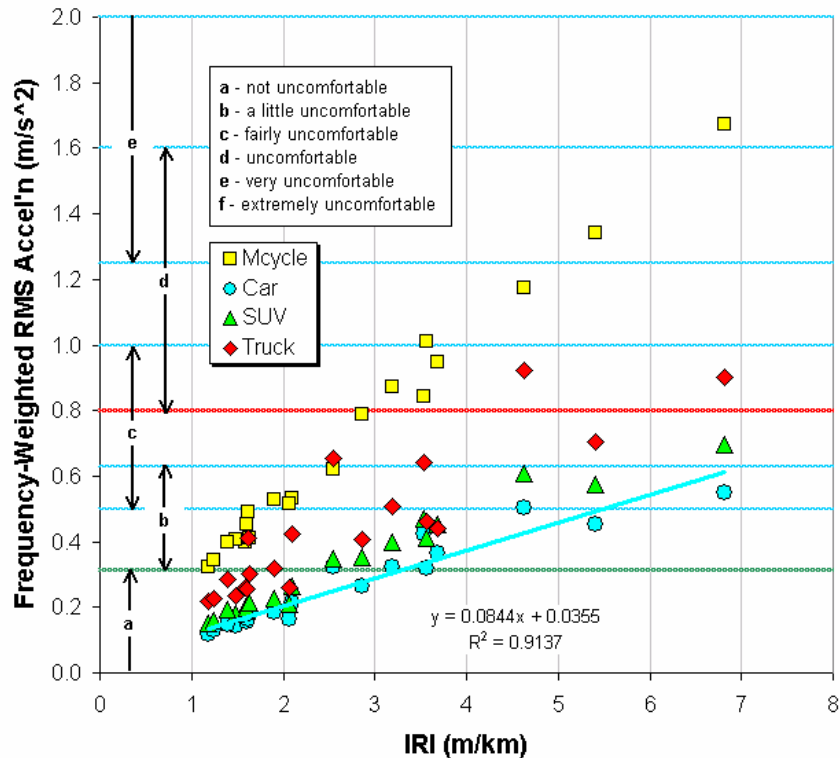


Figure 4. Ride model responses and likely reactions compared with the IRI.

Further Application of Ride Model

In order to determine if there were other pavement problem areas not apparent in the responses presented in Fig. 2 using the AABM measure and presentation format, the passenger-car ride model was used on the Lake George profiles to simulate ride vibration. The simulated ride vibration response is shown below in Fig. 5 together with the AABM trace from Fig. 2. The areas highlighted in Fig. 2 showing abrupt changes in the AABM are again circled, and three new areas of increased ride vibration response not apparent earlier are indicated in the plot with the bold yellow arrows. Though not readily apparent in the AABM plots, these areas of the pavement

would be likely to have a detrimental impact on the occupants' perception of ride quality and would benefit from grind treatment.

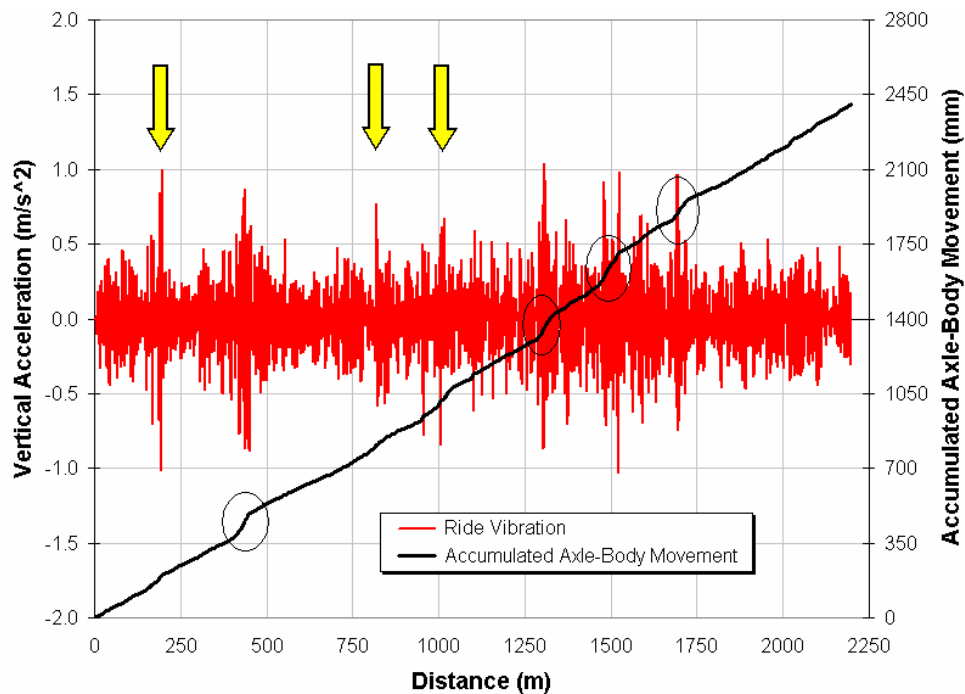


Figure 5. Ride vibration and IRI responses to the Lake George profiles.

Grinding Model and Profile Remediation

The profile analysis tools and ride models presented in the previous sections of this paper have been used to identify and locate pavement problem areas in example profiles. Further software tools were developed, in the form of numerical models that simulate conventional grinding equipment, in order to evaluate the potential effectiveness of grind treatments, as described below.

Grinding Basics. Profile grinding is generally accomplished using diamond grinding equipment, consisting of closely spaced diamond tipped blades mounted on a horizontal shaft known as a cutting or grinding head. The grinding head is mounted under a machine purpose-designed for this type of work. One example of a grinding machine, designed for production grinding of large pavement surfaces such as highways, runways and vehicle test pads, is shown below in Fig. 6.

The basic components of the grinding machine are identified below in Fig. 7. When operating, the front wheels of the machine (the small wheel-set at the right-hand end of the machine) pass over the bump or fault on the pavement surface and the cutting or grinding head, just to the right of the operator shown in Fig. 6, smooths the profile by grinding away the irregularities. The small wheel set for depth control located at the rear of the subframe, which supports the grinding head, tracks in the smoothed path as shown (see Fig. 7).



Figure 6. Large pavement grinding machine (from <http://www.boartlongyear.com>)

Various controls are used to regulate the depth of the grind, and its smoothing characteristics are determined by the position of the grinding head between the leading bogie and the depth control wheels, as described in more detail and demonstrated in the next section.

Grind Treatment Modelling. A numerical model was developed to simulate the pavement-grinding machine and implemented in the custom software *PaveGrind*TM. The basic features and key dimensions of the grinding machine used in the grinding algorithm are the wheelbase, L , and the location of the grinding head relative to the depth control wheels, αL , as illustrated in Fig. 7.

Other parameters that can be adjusted in the software are the grind head diameter, G , the interaction between the untreated profile and the leading bogie through dimension $B1$, interaction between the treated profile and the depth-control bogie, $B2$, and the height of the grind head relative to the subframe (grind depth, D), as illustrated in Fig. 7.

When applied to select user-defined segments of a profile, *PaveGrind*TM computes the height of the grinding head above or below the profile at each profile point. A grind treatment is only applied and profile modified if the grinding head is below the profile.

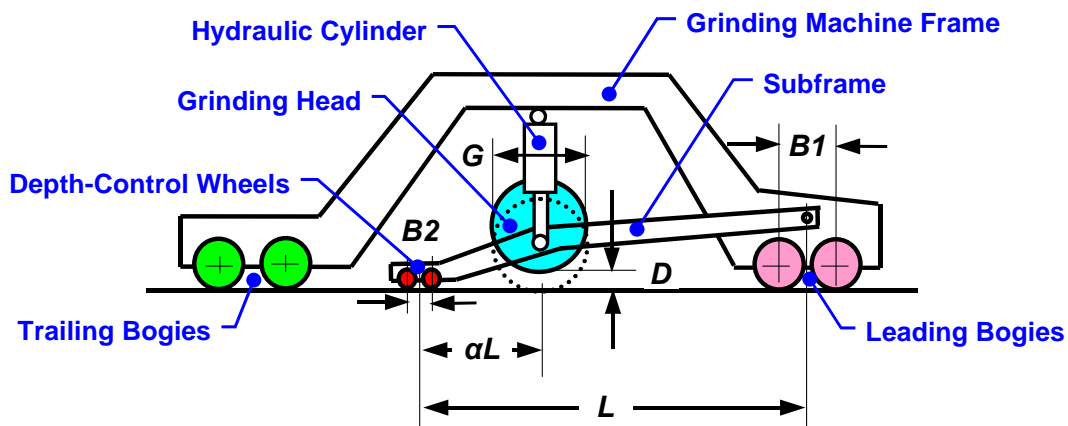


Figure 7. Basic components and schematic of the *PaveGrind*TM numerical model.

Fig. 8 illustrates the smoothing effect of a basic grinding algorithm (grind head making point contact with the profile) on a 24 m long, 5 mm step-up/down profile for a range of grinding head fore-aft locations, αL , on a grinder wheelbase, L , of 4 m. It can be seen that a more rearward location of the grinding head removes more material and produces a smoother profile.

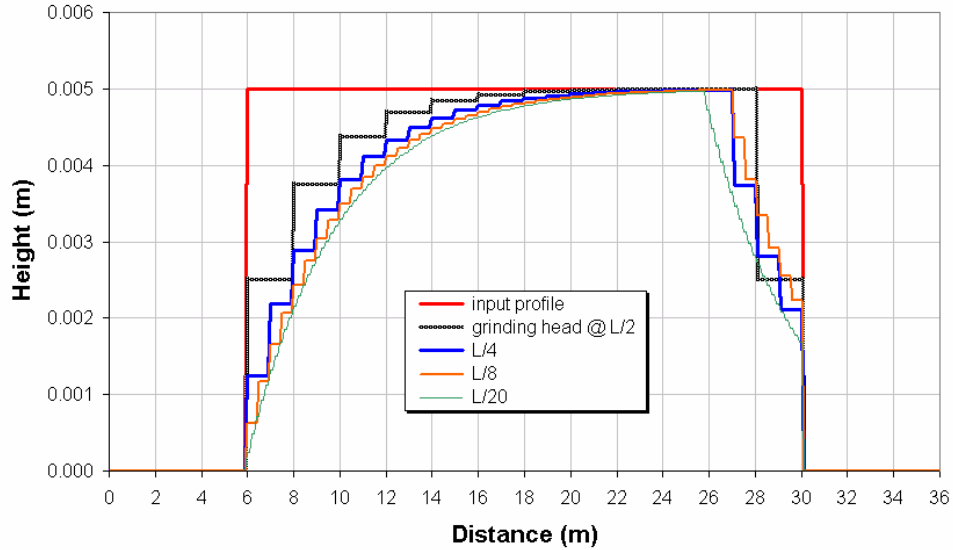


Figure 8. Smoothing characteristics of the basic *PaveGrind*[™] model.

Grind Treatment Application and Effectiveness. The *PaveGrind*[™] software and the effectiveness of profile remediation by grind treatment were evaluated on the Lake George profiles. Grind treatments were applied to the specific areas identified in Fig. 5 through the roughness measures of AABM, instantaneous IRI, and the frequency-weighted rms vertical acceleration. Only a single pass of the basic grinder over each section was made and the treatment lengths were not optimised.

The roughness measures and ride vibration estimates before and after virtual profile remediation are displayed in Fig. 9. The simulation indicates the pavement grinding treatment would be effective in reducing the overall IRI roughness by about 13% (from 1.095 to 0.952 m/km IRI) and improving the overall ride quality, as perceived by occupants of a conventional passenger car, by about 10.0% (reducing the ride vibration from 0.241 to 0.219 m/s²).

New Construction CRC Pavement

To further demonstrate the ride and grind numerical models, road profiles taken with an ARRB TR high-speed laser profiler on recently constructed CRC pavement of the West Charlestown Bypass in Newcastle (New South Wales, Australia) were analysed. Being new construction the roughness levels were low. The profiles were subdivided into 500 m equal length lots and simulations with the four ride models were performed. The overall ride vibration estimates and the corresponding IRI roughness

values are shown below in Fig. 10. Also shown are the ISO 2631-1 and BS 6841 comfort thresholds and RTA R83 QA incentive/deduction bands (Roads and Traffic Authority, 2002b). Under the RTA scheme, pavement segments which score a positive (+) value will earn an incentive payment, segments which score a negative (-) value are deemed non-conforming and, subject to certain further conditions may require surface grinding.

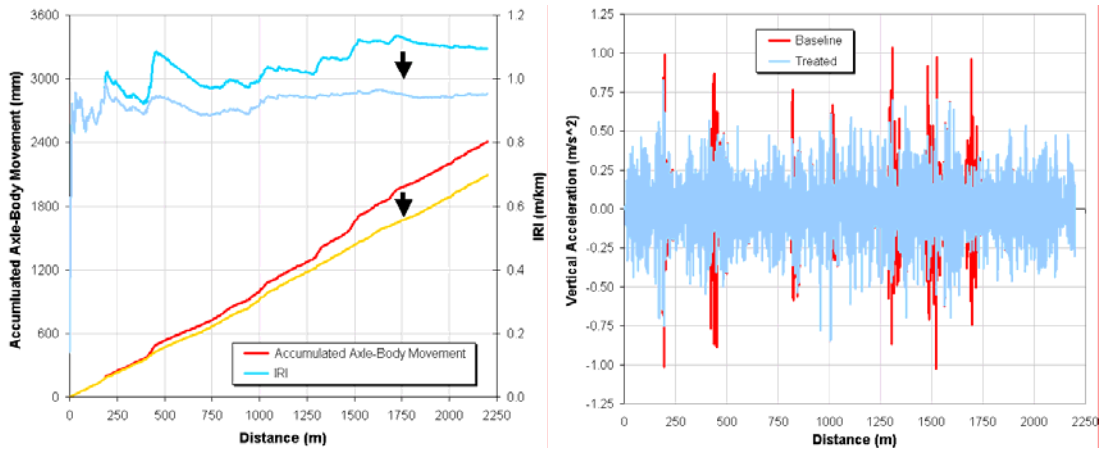


Figure 9. Various IRI and ride vibration responses before and after grind treatment.

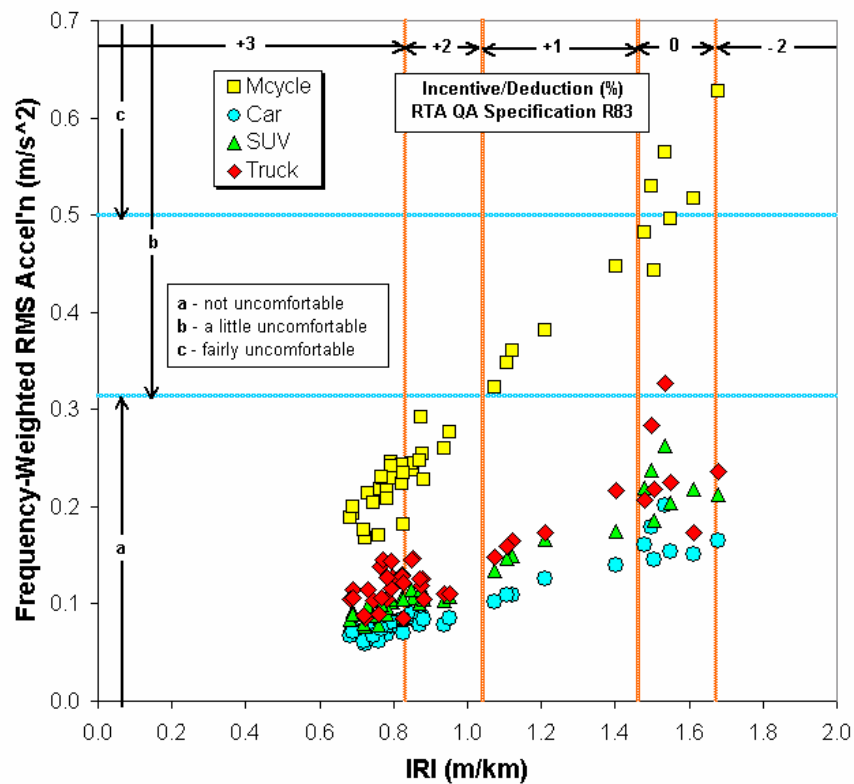


Figure 10. Baseline ride vibration estimates and IRI on new CRC pavement.

The results show that, based on the IRI, all segments would be considered acceptable and a number would earn incentive payments. Consistent with the RTA scheme, the outputs from the ride models suggest the ride quality would be acceptable for cars, SUVs and trucks but may be unacceptable for motorcycles on the segments having IRI roughness greater than 1.0 m/km. On these segments the ride quality would be rated by riders as “a little uncomfortable” to “fairly uncomfortable”.

The tools described earlier in this paper were applied to the profiles and the problem areas were identified and grind treatments applied where necessary. The ride simulations were rerun on the treated profiles leading to the results shown in Fig. 11, showing reductions in ride vibration to acceptable levels for all four vehicles, and all pavement segments scoring at least two positive (+) values, leading to overall higher incentive payments.

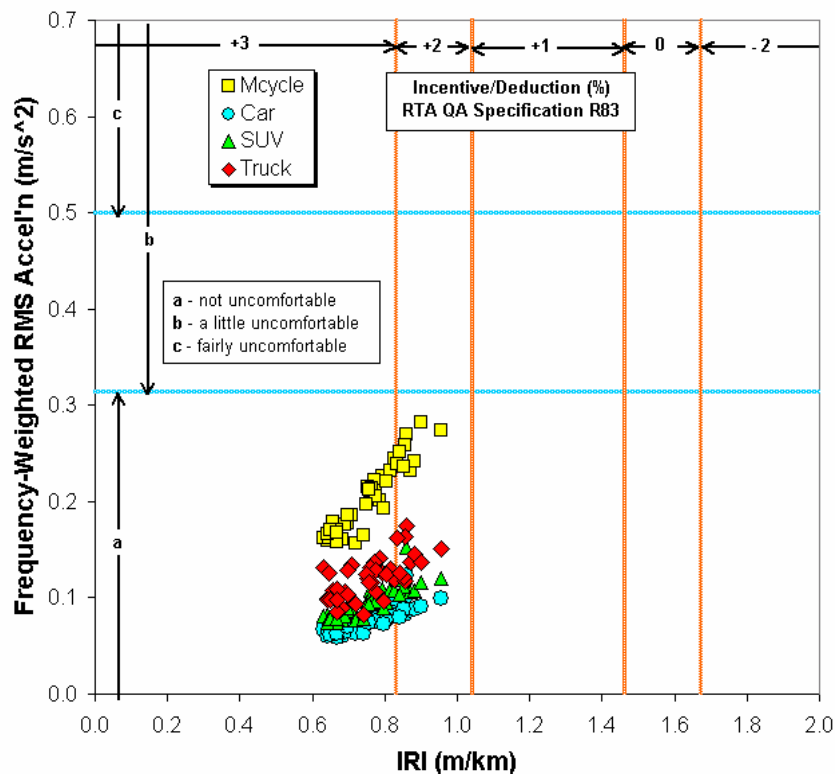


Figure 11. Ride vibration estimates and IRI after grind treatment on CRC pavement.

Intrinsic Unevenness

It was observed earlier that the rate of axle-body movement accumulation with distance of the IRI quarter-car is reasonably constant outside of areas containing discrete roughness features and profile imperfections. This characteristic was referred to earlier as intrinsic unevenness, reflecting as it does the underlying fundamental aspects of the paving process (equipment, crew, material properties, environmental factors, etc.). The concept of intrinsic unevenness is both introduced

and put forward, as described in this paper, as a useful metric for benchmarking and evaluating road pavers and road paving processes.

The following further examples demonstrating intrinsic unevenness were taken from the profiles recorded on the West Charlestown Bypass CRC pavement referred to earlier. They provide some useful observations and performance characteristics specific to stringline guided slip-form paving. The profiles and analysis results are presented in day-paved lots and contain each of four wheelpaths of the two-lane carriageway.

Fig. 12 shows the AABM on a pavement section having uniform and low intrinsic unevenness along its entire length in all four wheelpaths and two discontinuities at the start and end-of-day construction joints. Between the joints, axle-body movement accumulation can be seen to increase steadily at about 300 mm for every 500 m of distance paved. This trend is consistent across all four wheelpaths. If continued at this rate, the AABM at the end of 1000 m of paved distance would be 600 mm. Therefore, the intrinsic unevenness for this day-paved lot is estimated to be about 0.6 mm/m (0.6 m/km). This value approaches what is considered to be the best achievable with this type of slip-form paver under the prevailing conditions. It is also important to note that this value ignores the contribution from the construction joints at the start and end of the day's paving identified in Fig. 12. If the construction joints are included, the IRI values across the four wheelpaths are in the range 0.69 to 0.75 m/km.

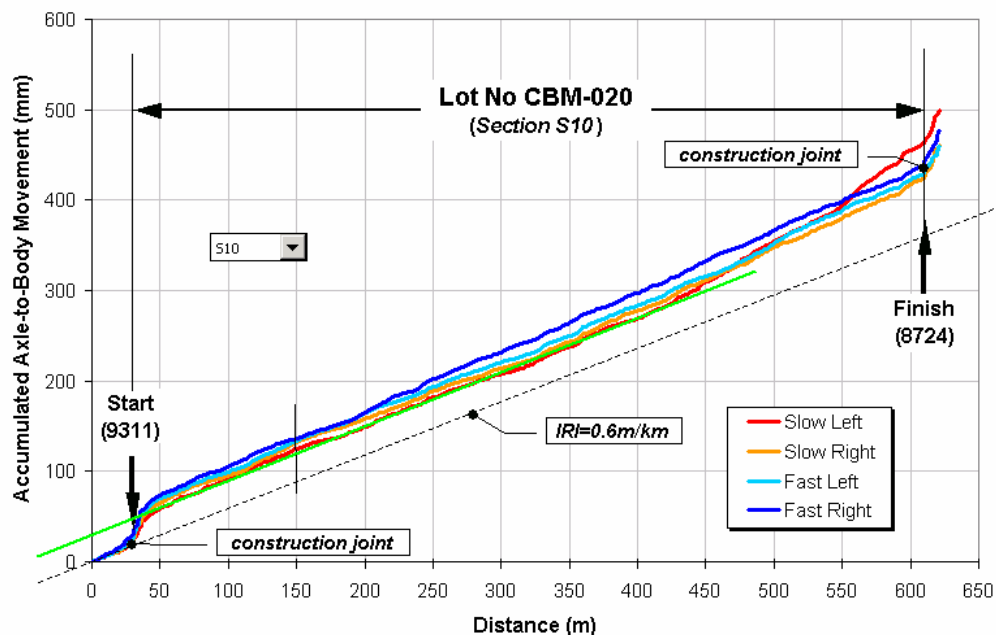


Figure 12. Smoothest day paving of the West Charlestown Bypass CRC pavement.

In the second example, shown in Fig. 13, delays in the paving operation led to stop/start interruptions over the middle segment, as indicated, increasing the intrinsic unevenness on that section from about 0.6 m/km at the beginning of paving to about 2.0 m/km. However, once paving was again underway, but without delays, intrinsic unevenness returned to that achieved at the beginning of the day. This suggests that stop/start interruptions appear to have a significant and detrimental influence on intrinsic unevenness.

Overall, taking all the profiles from the West Charlestown Bypass, it was observed that intrinsic unevenness could vary from day to day, along substantial sections within a day's paving, and across wheelpaths. The highest intrinsic unevenness generally occurred in one or both of the outer-most wheelpaths, ie in the slow-lane left and/or the fast-lane right wheelpaths. This can be seen in the example shown in Fig. 13. This is believed to be a direct result of the paver's levelling action, causing one or both sides of the paver main platform to rise or fall in response to levelling commands from the string line follower. These up and down movements would have the greatest influence on the outer-most wheelpath profiles. This was observed in the results from almost all of the day-paved sections. Path curvature effects (horizontal alignment and steering) may have similar adverse influences.

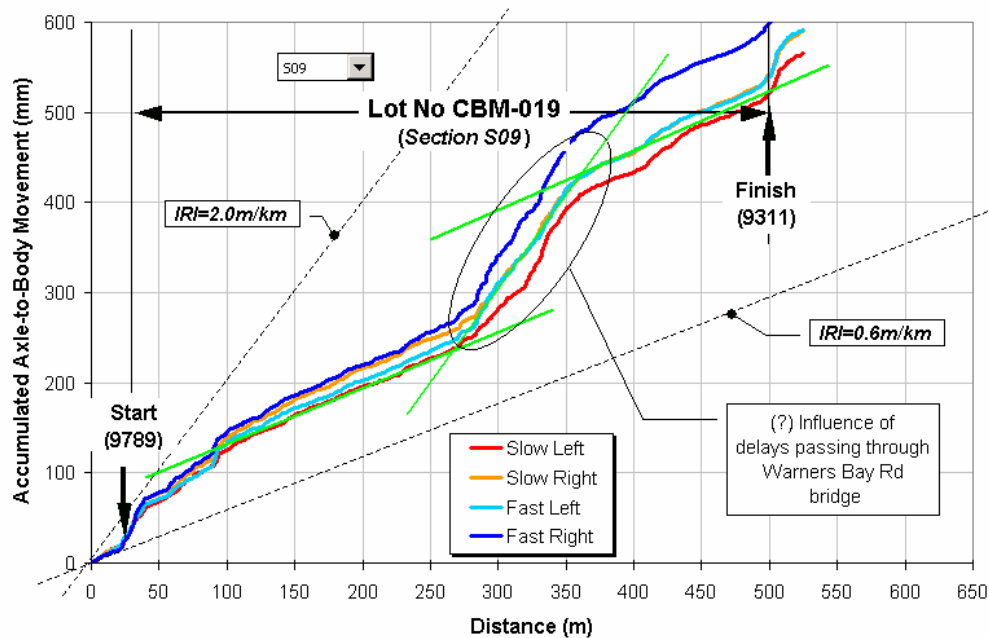


Figure 13. Paving delays causing a significant increase in intrinsic unevenness.

Other Factors Influencing Ride

Two other factors of interest related to CRC pavements and slip-form paving have been raised by this study, which are summarised in the sequence shown in Fig. 14.

Spectral analysis of road profiles, as used in other road paver studies (see Prem, 1989b), revealed the existence of two periodic components, shown in the top left of Fig. 14, that create unpleasant vibration to motorists. The first component, occurring at the lower wave number (identified as Spike A in Fig. 14), is thought to be associated with the setup of the string lines, which control the slip-form paver. The spacing of the support hubs is commonly around 7.5 m, whose inverse of 0.13 (1/7.5) equals the wave number shown in Fig. 14. It suggests that selecting a hub spacing that is out of phase with the sensor spacing on the paver could eliminate this irregularity.

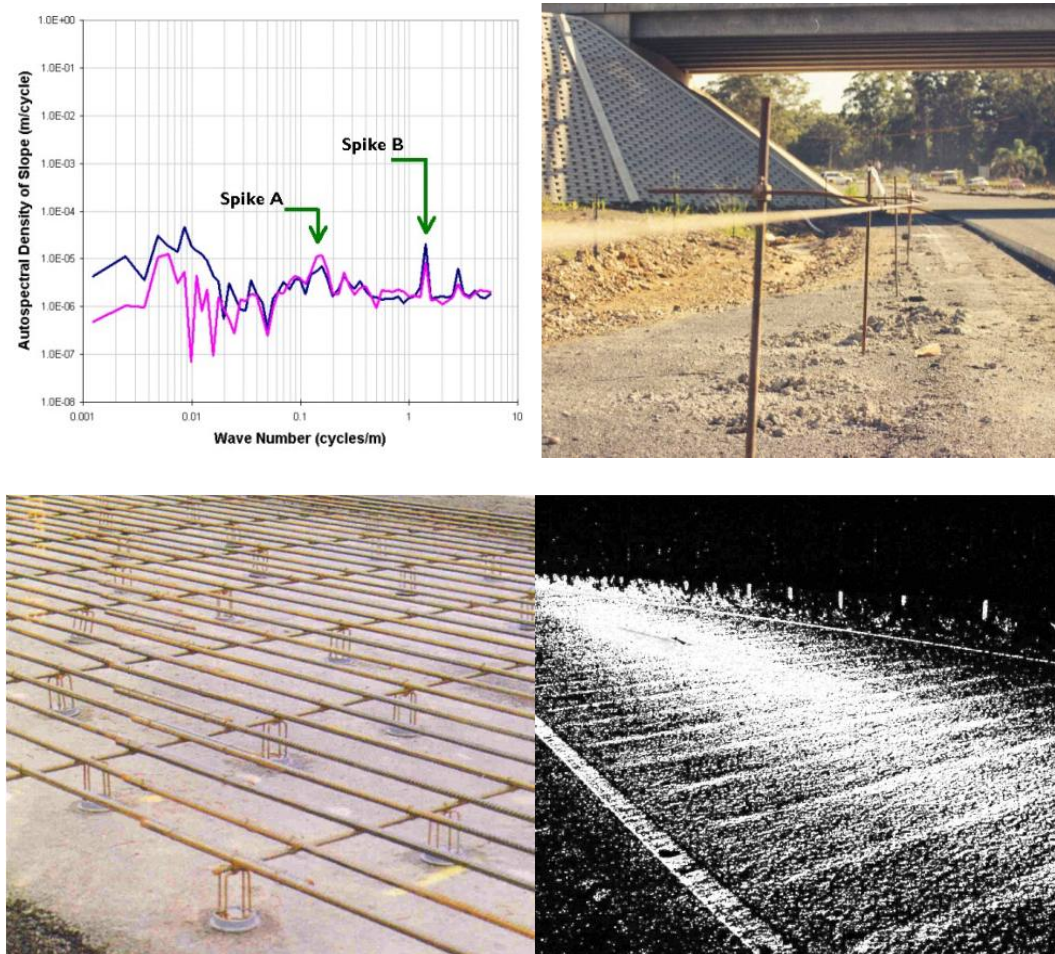


Figure 14. Other factors influencing ride.

The second periodic component, which occurs at the higher wave number (Spike B), is related to the spacing of transverse reinforcement in CRC pavements; see images at lower left and right of Fig. 14. The lower left plot shows the typical reinforcement in CRC pavements, the lower right plot shows the surface of CRC pavement as photographed at night under headlights. The bumps on the surface reflect the transverse bars and are thought to be caused by plastic settlement of the concrete. They are generally not detectable in daylight (even under a straight-edge),

but are noticeable to motorists, especially in SUVs, trucks and on motorcycles, as a low-level rumble⁵ vibration.

Both of these issues will be investigated further in the next stage of this project.

Summary

A range of new profile analysis tools and methods have been presented in this paper to help identify pavement problem areas in respect of rideability and to investigate remedial treatments using conventional pavement grinding equipment. The tools are based on numerical modelling and simulation, drawing on existing road surface unevenness and rideability indicators, such as the IRI, and new models that provide realistic estimates of ride vibration and perception of that vibration by humans.

The ride model was used to simulate the ride responses of a generic passenger car, a heavy commercial vehicle (truck), an off-road recreational and sports utility vehicle (SUV), and a motorcycle. By way of example, using road profiles measured on both flexible and rigid pavements, the predictive capability of the improved ride indicator was tested and the effectiveness of the tools was demonstrated. Numerical modelling of conventional grinding processes was also demonstrated and improvements in ride quality through virtual grind treatment were quantified.

The concept of intrinsic unevenness was introduced and put forward as a useful metric for benchmarking and evaluating road pavers and road paving processes.

In the next stage of this project, further investigations into slip-form pavers and new construction is planned, to identify and help control process related factors that have an adverse impact on road profiles and ride quality. In addition, the new profile analysis tools and ride indicators will be used to develop a better understanding of the relationship between specific road profile features and ride quality, and tested widely to assess their effectiveness in predicting pavement rideability.

References

Al-Omari, B. and Darter, M. I. (1994) "Relationships Between International Roughness Index and Present Serviceability Rating." *Transportation Research Record* 1435, TRB, National Research Council, Washington, D.C., 199_, pp130-136.

Auff, A. A., Tyson, G. and Choummanivong, L. (1995) *Evaluation of the Road Roughness Measuring Capability of ARRB's Prototype Walking Profilometer*. Research Report ARR 266. ARRB Transport Research Ltd.: Vermont South, Vic.

⁵ Rumble is a low frequency below 50 Hz.

Austrroads (1992) *Pavement Design – A Guide to the Structural Design of Road Pavements*. Austrroads Publication AP-17/92. Austrroads: Sydney.

Austrroads (2000) *A Road Profile Based Truck Ride Index (TRI)*. Austrroads Publication AP-R177, A4, 55pp. Austrroads: Sydney.

Austrroads (2001) *Guidelines for Road Condition Monitoring; Part 1 – Pavement Roughness*. Austrroads Publication AP-G65.1/01, A4, 56pp. Austrroads: Sydney.

British Standards Institution (1987) *Measurement and Evaluation of Human Exposure to Whole-Body Mechanical Vibration and Repeated Shock*. British Standard BS 6841:1987. London: British Standards Institution.

Griffin, M. J. (1990) *Handbook of Human Vibration*. Academic Press Limited, London.

International Standards Organisation (1997) *Guide for the Evaluation of Human Exposure to Whole-Body Vibration*. International Standard ISO 2631-1:1997(E). (International Organisation for Standardisation: Geneva, Switzerland)

Leatherwood, J. D., Dempsey, T. K. and Clevenson, S. A. (1980) “A Design Tool for Estimating Passenger Ride Discomfort within Complex Ride Environments.” *Human Factors*, 22(3), pp291-312.

Prem, H. (1989a) *NAASRA Roughness Meter Calibration by the Road-Profile-Based International Roughness Index*. Australian Road Research Board. Research Report ARR 164. Vermont South, Vic.

Prem, H. (1989b). “A Comparative Study of Two Automated Road Paving Machines”. *Australian Road Research* 19(2), June 1989, pp109-128.

Roads and Traffic Authority (2002a). *Test Method T187 – Measurement of Ride Quality of Road Pavements by Laser Profiler*. Pavements Branch, Roads and Traffic Authority of New South Wales. Australia. February 2002.

Roads and Traffic Authority (2002b) *RTA QA Specification R83 – Plain Concrete Base*. Pavements Branch, Roads and Traffic Authority of New South Wales. Australia. Edition2/Revision 5, May 2002.

Sayers, M. W. (1995). “On the Calculation of International Roughness Index from Longitudinal Road Profile.” *Transportation Research Record* 1501, TRB, National Research Council, Washington, D.C., 1995, pp1-12.

Sayers, M. W., Gillespie, T. D. and Quiroz, C. A. V. (1986). *The International Road Roughness Experiment: Establishing Correlation and a Calibration Standard for Measurements*. World Bank Technical Paper Number 45.

Sayers, M. W. and Karamihas, S.M. (1998). *The Little Book of Profiling – Basic Information about Measuring and Interpreting Road Profiles*. The University of Michigan Transportation Research Institute, Ann Arbor, Michigan, USA. September 1998.